4. Late Miocene Southern Thermal Development and its Connection to Mediterranean Climate History - Diatom Evidences from ODP Sites 701 and 704

B. Censarek and R. Gersonde

Alfred Wegener Institute for Polar and Marine Research, Bremerhaven, Germany

(Submitted to Marine Geology)

4.1 Abstract

Late Miocene to Early Pliocene diatom abundance fluctuations of Ocean Drilling Program (ODP) Leg 114 Sites 701 and 704 from the Atlantic sector of the Southern Ocean are studied to describe the thermal development of the Southern Ocean and its relation to the Messinian Salinity Crisis (MSC). This study of Sites 701 and 704, which are exceptional in containing a continuous Messinian sequence, includes Late Miocene diatom biostratigraphies and revises the magnetostratigraphical interpretations. Biostratigraphical diatom occurrence datums are reconsidered revealing some diachronous occurrences. Relative paleotemperatures, which are derived from abundances of thermal conditions indicating diatoms, and individual abundance fluctuations of selected diatom taxa are used to delineate the thermal sea surface development.

Cold climatic conditions are determined for the period between 6.6 and 5.3 Ma and within seven short periods (each ca. 100 k.y.) of cold and five of warm surface water masses, which are partly interrupted by thermal balanced transition stages. The reconstructed thermal history enabled the determination of the development of the hydrographic frontal system considering additional results from ODP Leg 113 and 177 sites. A Paleo-Polar-Front was probably formed at around 8.6 Ma. At around 6.6 Ma hydrographic fronts may have reached recent latitudes and are displaced northward up to ca. 5.3 Ma.

A combination of glacio-eustatic processes and regional tectonic movements is often proposed as mechanism to induce the isolation and flooding of the Mediterranean basin and to control the deposition of evaporites during the MSC. Southern Ocean diatom occurrences and abundance fluctuations are correlated to the Mediterranean development providing evidences for glacial-eustacy processes, which are responsible for the onset of the Mediterranean isolation.

4.2 Introduction

The Middle and Late Miocene climate development is characterised by cooling, increasing latitudinal thermal gradients, ongoing ice sheet build up in Antarctica and the onset of glaciations in the northern hemisphere (Kennett, 1977; Barron et al., 1991; Larsen et al., 1994). The temporary closure of the Panama Isthmus and the lowering of the Greenland-Scotland Ridge had certainly a great influence on Late Miocene climate development (Collins et al., 1996a, b; Wright and Miller, 1996). It is speculated that an ocean circulation pattern close to the present-day situation was established (Censarek and Gersonde, subm. b). The other significant event during the Late Miocene period is the isolation and desiccation of the Mediterranean Sea, the so-called Messinian Salinity Crisis (MSC). Restricted salinity from the Mediterranean Sea water may have had a strong impact on the Atlantic circulation pattern (Haug and Tiedemann, 1998; Rahmstorf, 1998). Regional tectonic movements and sea level fluctuations, which are ascribed to Antarctic ice volume changes, are proposed as mechanisms leading to restriction and reflooding of the Mediterranean basin (Hsü et al., 1973; Benson et al., 1991; Kastens, 1992; Krijgsman et al., 1999; Hodell et al., 2001; Vidal et al., 2001). However, up to now it is under discussion, which mechanism was the dominant trigger. Evidences for Antarctic ice sheet build up caused the MSC via sea level changes can be derived from the thermal evolution of the Southern Ocean Water masses. However, Southern Ocean sediment records close to the Miocene-Pliocene boundary documenting the thermal history are usually incomplete due to hiatus occurrences. Ocean Drilling Program (OPD) Sites 701 and 704 represent two of the few Southern Ocean sediment cores containing a continuous Messinian sequence. We extracted the diatom record to estimate Southern Ocean climate development. Studies based on the abundance pattern and distributions of extinct diatoms have been completed successfully for the delineation of climate variability in Middle Miocene and Pliocene sections (Koizumi, 1990; Barron, 1986, 1992b, 1996). Censarek and Gersonde (subm. b) deduced thermal affinities of extinct Miocene Southern Ocean species, which enable the calculation of relative paleotemperatures (RPT) and allow the interpretation of diatom assemblages.

The Southern Ocean thermal evolution as derived from RPT and abundance patterns of selected diatom taxa are compared with the Mediterranean climate history revealing evidences of the glacio-eustatic influence on MSC steering. The diatom records from ODP Sites 689, 1088 and 1092, which are located lati-

tudinal across the Atlantic sector of the Southern Ocean, are used to delineate a relative movement pattern of hydrographical paleo-fronts.

This study further includes diatom biostratigraphies of Sites 701 and 704, which improves some diatom occurrence datums and revises the magnetostratigraphic interpretation of Clement and Hailwood (1991) and Hailwood and Clement (1991b).

4.3 Material and methods

4.3.1 Core locations, sample preparation and counting

Site 701(51°59,07´S, 23°12.73´W) is locatedon the western flank of the Mid-Atlantic Ridge, around 160 km east of the Islas Orcadas Rise, located in a water depth of 4636 m (Shipboard Scientific Party, 1988c)(Fig. 4.1). This southernmost location in the Polar Front Zone is placed on a deep-sea water gateway. Site 704 sediments were drilled in a water depth of 2532 m at the Meteor Rise (46°52.75´S, 07°25.25´E), which is located in the north of the present Polar Front Zone (Shipboard Scientific Party, 1988d)(Fig. 4.1). This core location is within a mixing zone of upper North Atlantic Deep Water (NADW) and Circumpolar Deep Water (CDW). Hole 701C is selected of two cores containing Late Miocene sediments at Site 701. At Site 704 we chose Hole 704B, which is the only core drilled down to Miocene sediments. Diatom abundance pattern of selected species from ODP Leg 113 Site 689 from the north-eastern Maud Rise (68°S), Leg 177 Sites 1092 and 1088 from the northern Meteor Rise (46°S) and from the Agulhas Ridge (41°S) was also considered (Shipboard Scientific Party, 1988a; Shipboard Scientific Party, 1999a, b; Censarek and Gersonde, subm. b). Together with Site 704, which is located ca. 60 sea miles southeast of Site 1092 and allows a direct comparison of determined diatom data, a latitudinal transect across the Southern Ocean is studied. Site 701 extends the investigated area to the west (Fig. 4.1).

For a quantitative and qualitative diatom study, microscope slides with randomly distributed microfossils were used. The cleaning of the sediment samples and the preparation of permanent mounts for light microscopy follows the approved technique developed at the Alfred Wegener Institute (Gersonde and Zielinski, 2000). Up to 400 diatom valves were counted per sample following the concepts proposed by Schrader and Gersonde (1978). For counting a Zeiss "Axioskop" microscope with apochromatic optics at a magnification of 1000× was used. The applied diatom taxonomy information is summarised in Censarek and

Gersonde (2002). Range charts showing stratigraphic occurrences and abundances of selected diatom species of Holes 701C and 704B are available at the PANGAEA database (http://www.pangaea.de). Diatom concentrations are calculated as diatoms per gram dry sediment. For ease of comparison all ages are tied to the current Geomagnetic Polarity Time Scale of Berggren et al. (1995).

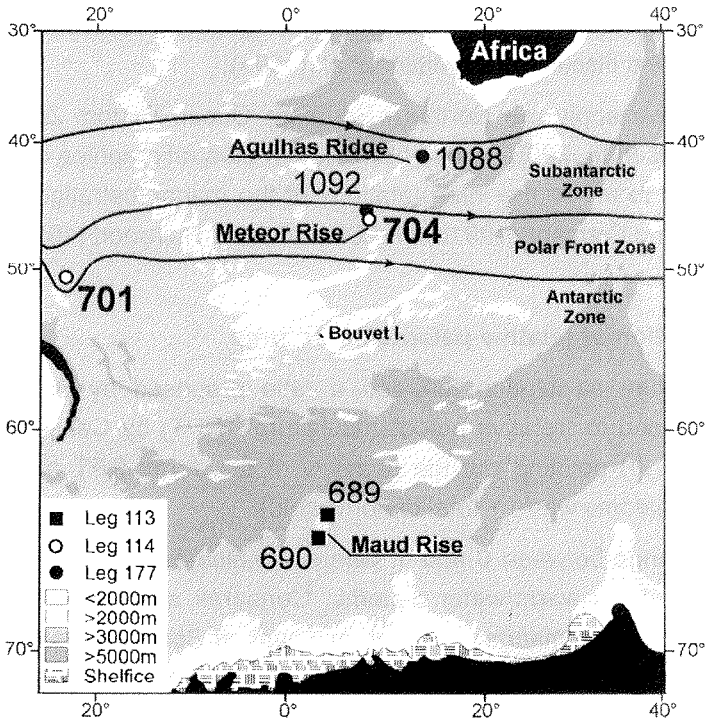

Figure 4.1: Location of ODP Sites 689, 701, 704, 1088 and 1092 in the Atlantic sector of the Southern Ocean. Frontal zones according to Peterson and Stramma (1991).

4.3.2 Chronology

Diatom biostratigraphies of the Miocene sediments recovered during Leg 114 were never published appropriately. The age control of the magnetostratigraphic interpretation at Site 701 is provided by a siliceous microfossil biostratigraphy (Ciesielski, 1991; Clement and Hailwood, 1991). For the Miocene sections of Hole 701C only shipboard diatom zone correlations are available (Shipboard Scientific Party, 1988c). The inclination record contains sections with

wide sample spacing (Shipboard Scientific Party, 1988c), which results in inaccurate chron boundaries and the lack of information about complete chrons.

Diatom abundance estimates at Hole704B associated with diatom zonations of Barron (1985a) and Weaver and Gombos (1981) are published in a data report (Ciesielski, 1991). Hailwood and Clement (1991b) presented a magnetostratigraphical interpretation of Hole 704B based on biostratigraphical datums, which are compiled and discussed by Müller et al. (1991).

In this study we apply the Northern Southern Ocean Diatom Zonation (Censarek and Gersonde, 2002) to establish diatom biostratigraphies of Holes 701C and 704B and to revise the interpretations of the magnetostratigraphic records by Hailwood and Clement (1991b) and Clement and Hailwood (1991).

4.3.3 Estimation of relative paleotemperatures

Paleotemperature calculation followed a ratio proposed by Barron (1992b), which is renamed to "relative paleotemperature" (RPT) by Censarek and Gersonde (subm. b) pointing out the relativity of this term: RPT = total diatoms warm / (total diatoms warm + total diatoms cold).

RPT values range between 0 and 1, where 0 indicates entirely cold-water diatoms and 1 entirely warm-water diatoms. Censarek and Gersonde (subm. b) derived the thermal demands of extinct taxa by their Southern Ocean and global geographical and stratigraphical distribution and by the co-occurrence with extant taxa, which is classified on direct observations. Further evidence of species thermal demands is gained by the affiliation to a genus that can be linked to a specific thermal environment.

The group of warm-water indicating diatom species considered in this study consists of *Actinocyclus ingens*, *A. ingens* var. *ovalis*, *Azpeitia tabularis*, *Fragilariopsis reinholdii*, *Hemidiscus cuneiformis*, *Hemidiscus karstenii*, *Hemidiscus triangularus*, *Thalassionema* spp. and *Thalassiosira oestrupii*. The *Thalassionema*-group includes *T. nitzschioides* var. *inflatum*, *T. nitzschioides* var. *lanceolatum* and *T. nitzschioides* var. *parvum*. The group of Southern Ocean cold-water indicating diatom species is composed of *Denticulopsis dimorpha*, *D. ovata*, *Fragilariopsis aurica*, *F. arcula*, *F. praecurta* and *F. donahuensis*.

4.3.4 Derivation of hydrographic front migration

Southern Ocean surface water evolution and hydrographic front development will be roughly outlined and discussed. The average locations of these hydrographic fronts are strongly linked to the topographic features of the Southern Ocean (Moore et al., 1999). However, Late Pleistocene studies revealed front displacements of a few latitudinal degrees northward during cold/glacial and southward during warm/interglacial stages (Morley and Hays, 1979; Prell et al., 1980; Brathauer, 1996, Brathauer and Abelmann, 1999). Barron (1996) estimated the Pliocene position of the Antarctic Polar Front based on selected diatom abundance fluctuations and suggested that frontal zones in the southeastern Atlantic may have migrated southward during the Pliocene warming over approximately 6° latitude. Therefore we interpret from an estimated cold stage a relative migration of surface waters northward and from a warm period a southward relative surface water movement. Comparisons of extant taxa abundances and of diatom concentrations with present-day ranges provide further evidences of water mass migrations.

4.4 Results

4.4.1 Diatom biostratigraphy and revision of the magnetostratigraphies of Holes 701C and 704B

Hole 701C

The uppermost investigated sediment section belongs to the *T. inura* Zone as indicated by the first occurrence (FO) of *T. inura* defining the lower boundary of the *T. inura* Zone (Fig. 4.2). This first occurrence datum (FOD) is found between samples 13H-2, 50-51cm and 13H-2, 149-150 cm (113.28 mbsf) representing an age of approximately 4.9 Ma. From this evidence it can be inferred that the normal polarised chrons around 110 and 115 meter below sea floor (mbsf) are Sidufjall (C3n.3n) and Thvera (C3n.4n). The underlying sediments belong to the *Hemidiscus triangularus - Fragilariopsis aurica* Zone (Fig. 4.2). The FO of *Thalassiosira oestrupii* is at 129.27 mbsf between samples 14H-6, 49-50 cm and 15H-1, 45-46 cm, which is in the lower to middle portion of Chron C3r (5.23 - 5.89 Ma) and coincides with the FO in Hole 704B. Baldauf and Barron (1991) derived at Sites 737A and 745B an age of 5.6 Ma for the FOD of *T. oestrupii*, which is in accordance with our results. For the section following below around ca. 137 up to 130 mbsf no magnetostratigraphical data are available (Shipboard Scientific Party, 1988c).

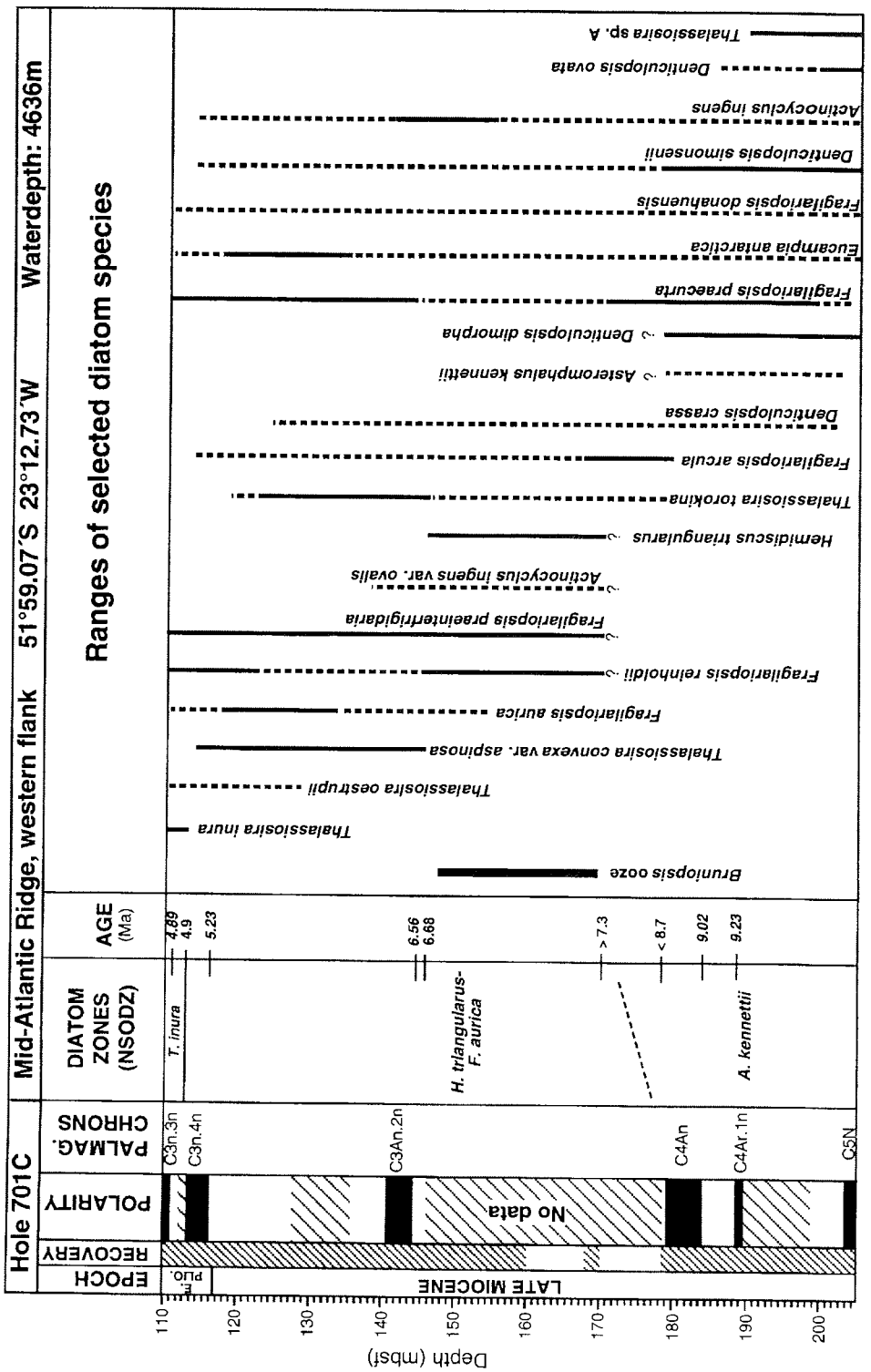
Hole 701C
Mid-Atlantic Ridge, western flank
51°59.07'S 23°12.73'W
Waterdepth: 4636m
EPOCH
RECOVERY
POLARITY
PALMAG. CHRONS
DIATOM ZONES (NSODZ)
AGE (Ma)
Ranges of selected diatom species
E. Plio.
LATE MIOCENE
No data
C3n.3n
C3n.4n
C3An.2n
C4An
C4Ar.1n
C5N
T. inura
H. triangularus-F. aurica
A. kennettii
4.89
4.9
5.23
6.56
6.88
> 7.3
< 8.7
9.02
9.23
Brunlopsis ooze
Thalassiosira inura
Thalassiosira oestrupii
Thalassiosira convexa var. aspinosa
Fragilariopsis aurica
Fragilariopsis reinholdii
Fragilariopsis praeinterfrigidaria
Actinocyclus ingens var. ovalis
Hemidiscus triangularus
Thalassiosira torokina
Fragilariopsis arcula
Denticulopsis crassa
Asteromphalus kennettii
Denticulopsis dimorpha
Fragilariopsis praecurta
Eucampia antarctica
Fragilariopsis donahuensis
Denticulopsis simonsenii
Actinocyclus ingens
Denticulopsis ovata
Thalassiosira sp. A
110
120
130
140
150
160
170
180
190
200
Depth (mbsf)

The next biostratigraphical datum point is the FO of *T. convexa* var. *aspinosa* (ca. 6.68 Ma) at 145.9 mbsf between samples 16H-5, 10-11 cm and 16H-5, 110-111 cm. This identifies the normal polarised interval around 143 mbsf as Chron C3An.2n. Accordingly it can be supposed that the missing Chron C3An.1n would be found in the magnetostratigraphical data gap above (Fig. 4.2). Between 170.1 and 145.90 mbsf a ca. 25 m thick *Bruniopsis*-ooze is located. Within this section the FO of the rare species *Fragilariopsis aurica* is found between samples 17H-4, 59-60 cm and 17H-5, 110-111 cm at 154.9 mbsf, which refers to an age somewhere in the range of 7.3 to 6.7 Ma. The *Bruniopsis*-ooze is interrupted by a recovery gap spanning from 160.20 to 168.10 mbsf. The missing time period can not be determined reliably due to the lack of nearby age control points, but, provided that sedimentation rates are linear, a gap of less than 0.1 Ma is suggests. Below the *Bruniopsis*-ooze a second recovery gap from 170.15 to 178.10 mbsf and spans the period from at least 7.3 to approximately 8.7 Ma. Sediments containing the lower portion of the *Hemidiscus triangularus* - *Fragilariopsis aurica* Zone and the complete *F. reinholdii*- and *Actinocyclus ingens* var. *ovalis* Zones are lacking due to the recovering gap.

The normal polarised intervals around 183 and 190 mbsf are interpreted as Chrons C4n and C4Ar.1n as indicated by the occurrence of *Asteromphalus kennettii* in absence of *Actinocyclus ingens* var. *ovalis*. This sediment section is in assignment to the *Asteromphalus kennettii* Zone. The co-occurrence of *A. kennettii* and *F. praecurta* reveals that underlying sediments up to at least 205 mbsf still belong to the *A. kennettii* Zone. This suggests that the long normal polarised interval at 204.01 mbsf (top) is Chron C5n (Fig. 4.2).

Age control points and the corresponding age-depth diagram are shown in Table 4.1 and in Figure 4.3. High sedimentation rates between 6.7 and 7.3 Ma can be deduced fromt the *Bruniopsis*-ooze occurrence. Remarkable in the Late Miocene section at Site 701C is the continuous occurrence of *Eucampia antarctica* reaching abundances close to the present-day range in this geographical area (Zielinski and Gersonde, 1997).

Figure 4.2 (left): Stratigraphic ranges of selected diatom species in the Late Miocene section of Hole 701C. Dotted lines indicate scattered and trace occurrences of diatom taxa. The diatom zonal assignment tied to the geomagnetic data of Clement and Hailwood (1991) is based on the Northern Southern Ocean Diatom Zonation (NSODZ)(Censarek and Gersonde, in press). Italic style ages are derived by magnetostratigraphy, normal style ages present diatom ages points.

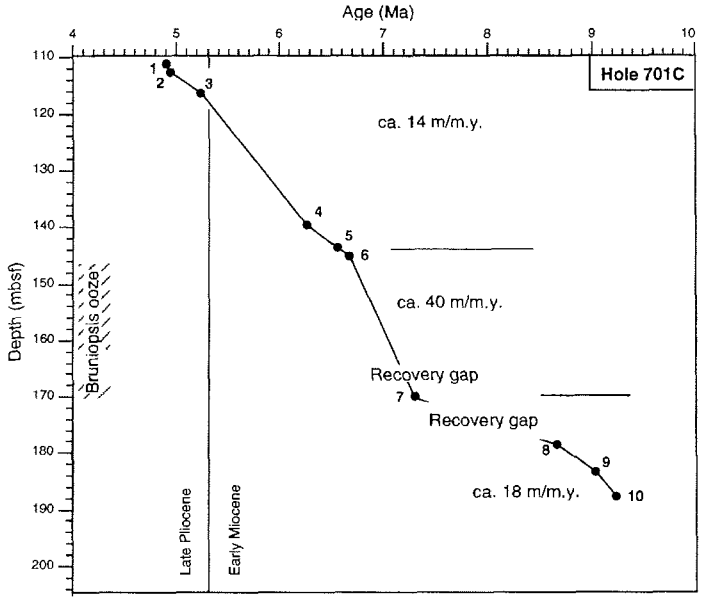

Figure 4.3: Age-depth diagram for the Late Miocene section of Hole 701C and calculated average sedimentation rates. For definition of stratigraphic datum points see Table 4.1.

Table 4.1: Definition of stratigraphic datum points in the Late Miocene section of Hole 701C used to construct the age-depth diagram in Figure 4.3.

Datum points	Depth (mbsf)	Age (Ma)	Definition
1	111.2	4.89	Base C3n.3n
2	113.3	4.9	FOD *T. inura*
3	116.1	5.23	Base C3n.4n
4	140.27	6.27	Top C3An.2n
5	144.2	6.56	Base C3An.2n
6	145.9	6.68	FOD *T. covexa* var. *aspinosa*
	160.20-168.10	Recovery gap	
7	170.14	7.3	FOD *H. triangularus*
	170.15-178.10	Recovery gap	
8	179.07	8.67	Top C4An
9	183.98	9.02	Base C4An
10	188.24	9.23	Top C4Ar.1n

Thalassionema sp. A occurred during Chron C3r (Fig. 4.2) in a short period of 300 k.y. and it might possibly be used in future to refine Late Miocene diatom zonations. This species has a bone like outline and further taxonomical and biogeographical studies are needed to evaluate its significance as stratigraphic marker. High abundances of the *Stephanopyxis* species occurred close to the Miocene/Pliocene boundary. This finding is in accordance with results from Leg 119 Site 737, which is located also close to the Polar Front within the Antarctic Zone (Baldauf and Barron, 1991).

Hole 704B

The uppermost portion of studied sediments belongs to the *T. inura* Zone. *Thalassiosira inura* occurs first between samples 24X-6, 53-54 cm and 24X-6, 129-130 cm at 222.11 mbsf, which corresponds to Chron C3r (Fig. 4.4). However, the FO of *T. inura* is generally observed within Chron C3n.3r at ca. 4.9 Ma (Censarek and Gersonde, 2002). To solve this discrepancy a short-term hiatus at around 222 mbsf omitting C3n.4n might be assumed. A comparable situation is documented at Site 1092 (Censarek and Gersonde, 2002). However, the normal polarised interval at 219 mbsf would belong consequently to Chron C3n.3n, which would lead to an unrealistic sedimentation rate of ca. 48 m/My during the Gilbert Chron (Fig. 4.4). The Gilbert Chron is well documented at the base of Hole 704A as well as at the top of Hole 704B (Hailwood and Clement, 1991b). Comparison with Site 1092 abundance fluctuations of *F. praecurta*, *F. fossilis*, *T. oestrupii* as well as comparison of the diatom sedimentation rate provide no evidences for a hiatus spanning the upper Messinian sediments. Therefore, we agree with the magnetostratigraphic interpretation of Hailwood and Clement (1991b). The FOD of *T. inura* is only well documented at the Maud Rise sediments (Censarek and Gersonde, 2002) and at Site 701 (this paper). At other sites close to the southern Polar Front boundary the FO of *T. inura* is generally found somewhere in the middle portion of the Gilbert Chron (Censarek and Gersonde, 2002). We assume that *T. inura* occurs somewhat earlier (ca. 5.2 Ma) in the northern part of the Polar Front Zone. Unfortunately no other corresponding sediment sections from this hydrographical region are available to prove this assumption. More investigations are needed to improve and clarify the diatom biostratigraphy at the Miocene/Pliocene boundary. Between samples 27X-6, 1-2 cm and 27X-6, 83-84 cm at 250.12 mbsf the FO of *Hemidiscus triangularus* (7.3 Ma) indicates the base of the *Hemidiscus triangularus* - *Fragilariopsis aurica* Zone (Fig. 4.4).

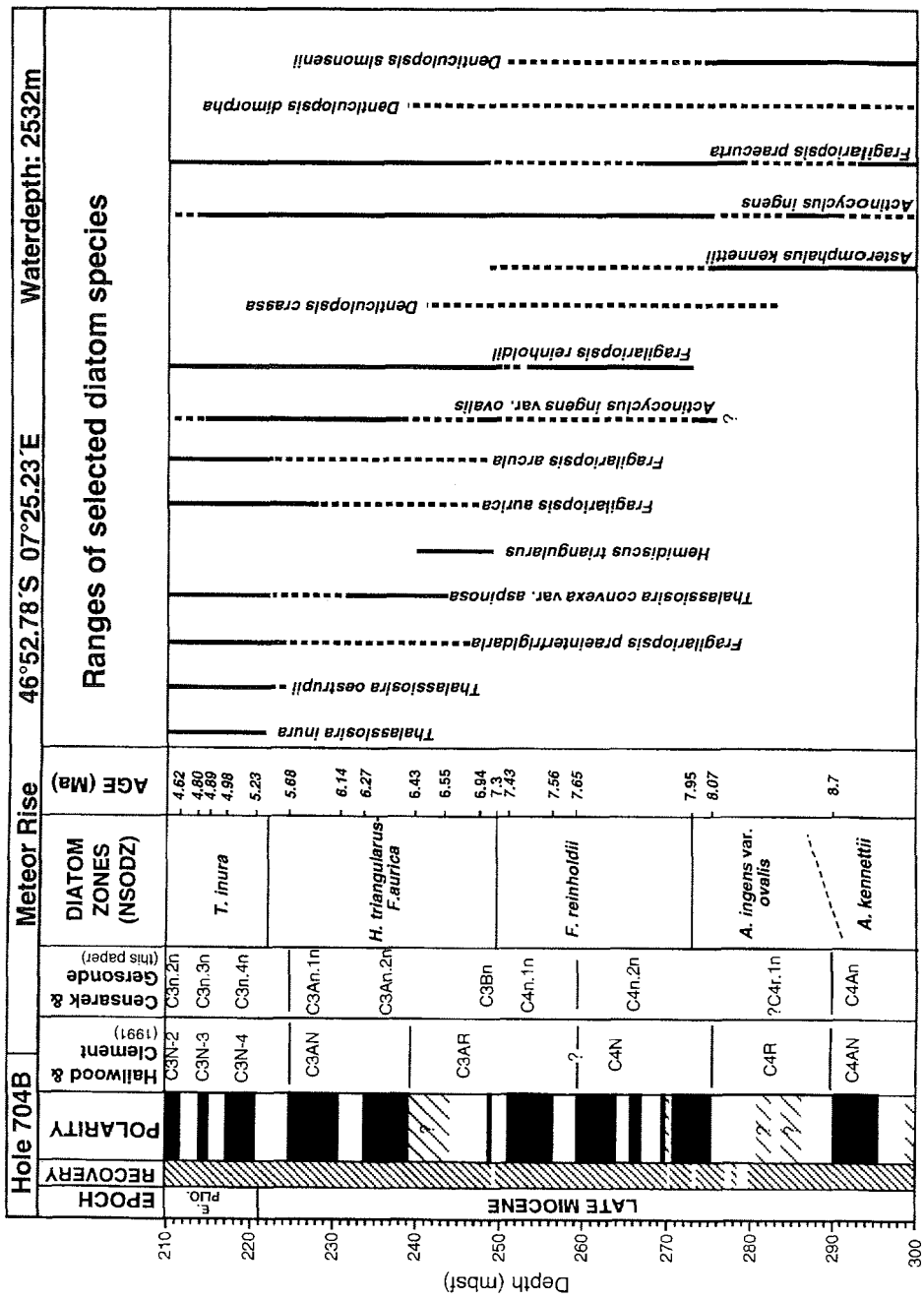

Figure 4.4: Stratigraphic ranges of selected diatom species in the Late Miocene section of Hole 704B. Dotted lines indicate scattered and trace occurrences of diatom taxa. The diatom zonal assignment based on the Northern Southern Ocean Diatom Zonation (NSODZ)(Censarek and Gersonde, 2002) is tied to the geomagnetic data of Hailwood and Clement (1991b). Italic style ages are magnetostratigraphic age points, normal style ages present diatom ages points.

This zone comprises Chrons C3Bn up to C3An.1n. As indicated by the FO's of *F. aurica* and *H. triangularus* we identified Chron C3Bn, which differs from the interpretation of Hailwood and Clement (1991b) who interpreted this interval as a portion of Chron C3Ar (Fig. 4.4). The FO of *Thalassiosira oestrupii* (ca. 5.8 Ma), occurring in the upper portion of the *H. triangularus* - *F. aurica* Zone, is found between samples 25X-1, 93 cm and 25X-2, 18-19 cm and corresponds to Chron C3r (Fig. 4.4). This is comparable to findings in Hole 701C (this paper) and Leg 119 Site 745 (Baldauf and Barron, 1991). The FO of *F. reinholdii* is found between samples 30X-2, 71-72cm and 30X-3, 84-85cm (273.7 mbsf), marks the lower boundary of the *F. reinholdii*-Zone and suggests an age of ca. 7.95 Ma. This led us to term the normal polarised interval at around 273 mbsf as the lowermost portion of Chron C4n.2n (Fig. 4.4). Consequently, the normal polarised interval above (around 255 mbsf) is Chron C4n.1n. Low inclination values between 265 and 272 mbsf (Hailwood and Clement, 1991b, fig. 12) indicate that this portion might also belong to Chron C4n.2n. The lower boundary of the underlying *A. ingens* var. *ovalis* Zone is defined by the FOD of the this species, which cannot be determined reliably due to rare occurrences. This finding differs from Site 1092 where this boundary is clearly found (Censarek and Gersonde, 2002). However, the common occurrence of *A. kennettii* up to ca. 277 mbsf (upper portion of Chron C4r) identifies the normal polarised Chron around 293 mbsf as C4An (Fig. 4.4) according to Hailwood and Clement (1991b). Age control points and the corresponding age-depth diagram are shown in Table 4.2 and at Figure 4.5.

Stratigraphic results of both holes verify known FOD's and reveal possible diachronous occurrences of *T. inura*. Most of the stratigraphically useful FOD's of Hole 704B (*F. reinholdii*, *T. convexa* var. *aspinosa*, *H. triangularus* and *F. aurica*) verify the interpretation at Site 1092 (Censarek and Gersonde, 2002) and are also comparable to occurrences documented in the data report of Ciesielski (1991). All new and revised estimates of first and last occurrence datums at Sites 701 and 704 are listed in Table 4.3. Our magnetostratigraphic interpretation of Hole 701C is in agreement with those published by Clement and Hailwood (1991). We also confirm most of the magnetostratigraphic interpretations of Hole 704B by Hailwood and Clement (1991b), but suggest a slightly older age (ca. 0.3-0.5 m.y.) for the section between ca. 240 and 260 mbsf. The FOD's of *Thalassiosira convexa* var. *aspinosa* and *Hemidiscus triangularus* revised the interpretation of Hailwood and Clement (1991b) from Chron C3Ar to Chron C3Bn and C4n.1n.

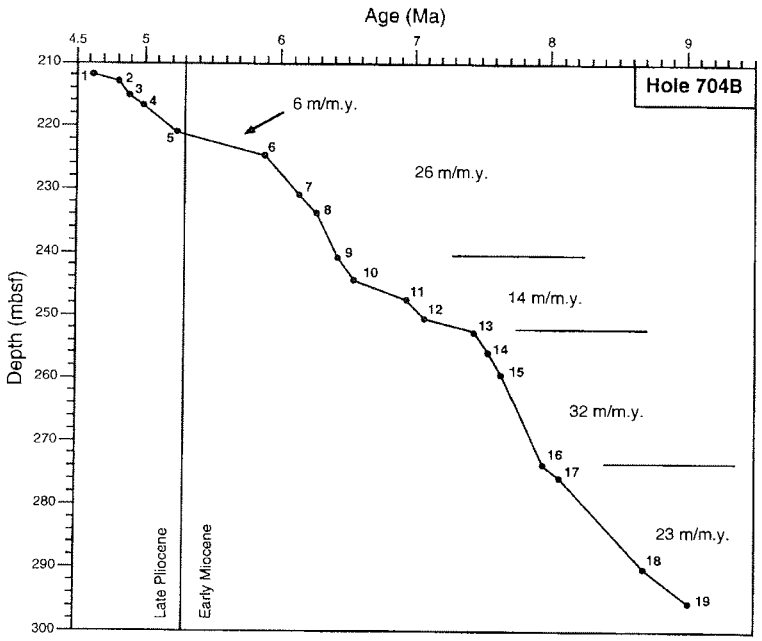

Figure 4.5: Age-depth diagram for the Late Miocene section of Hole 704B and calculated average sedimentation rates. For definition of stratigraphic datum points see Table 4.2

Table 4.2: Definition of stratigraphic datum points in the Late Miocene section of Hole 704B used to construct the age-depth diagram in Figure 4.5

atum points	Depth (mbsf)	Age (Ma)	Definition
1	212.00	4.62	Base C3n.2n
2	213.90	4.8	Top C3n.3n
3	215.30	4.89	Base C3n.3n
4	216.80	4.98	Top C3n.4n
5	220.80	5.23	Base C3n.4n
6	224.76	5.88	Top C3An.1n
7	231.04	6.14	Base C3An.1n
8	233.84	6.27	Top C3An.2n
9	240.88	6.43	LOD *H. triangularus*
10	244.52	6.55	FOD *T. convexa* var. *aspinosa*
11	247.71	6.94	FOD *F. aurica*
12	250.12	7.3	FOD *H. triangularus*
13	251.25	7.43	Top C4n1.n
14	256.75	7.56	Base C4n1.n
15	259.50	7.65	Top C4n.2n
16	273.73	7.95	FOD *F. reinholdii*
17	275.85	8.07	Base C4n.2n
18	290.07	8.7	Top C4An
19	295.60	9.02	Base C4An

Table 4.3: List of selected Late Miocene diatom events at Sites 701 and 704. The ages are interpolated by linear relationship from the age-depth plots. Additionally, diatom occurrence datums from previous studies at Sites 689, 1088 and 1088 are listed (Censarek and Gersonde, 2002). Italic style: low reliability. AZ: Antarctic Zone; SPFZ: Southern Polar Front Zone; NPFZ: Northern Polar Front Zone; SAZ: Subantarctic Zone.

Datums	Estimated diatom ages (Ma)					
	AZ		SPFZ	NPFZ		SAZ
	689B	690B	701	704	1092	1988
FOD *T. inura*	4.89	-	**5.00**	***5.54***	-	4.17
FOD *F. praeinterfigidaria*	5.09	-	**6.70**	**6.84**	-	-
FOD *T. oestrupii*	-	-	***5.80***	***5.84***	-	-
LOD *H. triangularus*	5.13	-	**6.60**	**6.43**	6.43	-
FOD *Thal. convexa* var. *aspinosa*	6.58	-	**6.66**	**6.57**	6.54	-
FOD *H. triangularus*	7.30	-	-	**7.29**	7.30	-
LOD *D. crassa*	*7.39*	*7.76*	***5.62***	***6.43***	7.51	-
FOD *F. reinholdii*	-	-	***7.3-8.5***	**7.96**	7.96	*8.23*
FOD *F. arcula*	8.49	8.41	***8.78***	***7.06***	*7.40*	-
FOD *A. ingens* var. *ovalis*	*8.49*	-	***7.3-8.5***	***8.10***	8.70	-
LOD *D. ovata*	*4.93*	-	**6.95**	***8.24***	10.60	*10.50*
FOD *F. aurica*	*9.50*	*10.30*	***6.91***	***6.94***	*6.94*	-

4.4.2 Diatom abundances and relative paleotemperatures

Abundance fluctuations of diatom taxa, which are used to estimate the relative paleotemperature, are presented in Figures 4.6 and 4.7. At Site 701 warm-water indicating species *Fragilariopsis reinholdii*, *Actinocyclus ingens* and *Azpeitia tabularis* characterise the assemblage between 7.3 and 6.7 Ma (Fig. 4.6). *Thalassionema nitzschiodies* and its varieties, which are also warm-water indicating diatoms, occurred at ca. 6.7 Ma and dominated the assemblage with abundances of up to more than 90%. At 5.7 Ma the warm-water species *Thalassiosira oestrupii* is also continuously present. However, higher abundances of *Fragilariopsis praecurta* document a cooling of cold surface waters between 6.7 and 5.7 Ma. Cold-water indicating *Eucampia antarctica* is frequently present at Site 701 with an abundance maximum at 5.5 Ma (Fig. 4.6). This maximum possibly correlates with a 2% abundance peak documented at Site 704, while this species is mostly absent from the rest of the Miocene core section (see datasheet).

The warm-water indicating diatom *Hemidiscus karstenii* could not be found at Site 701, whereas this species dominated the assemblage at Site 704 between ca. 9 and 8.1 Ma (Figs. 4.6, 4.7). The also warm-water indicating diatom *Actinocyclus ingens* occurred at Site 704 between 8.1 and 7.4 Ma with abundances of up to 80% and replaced *H. karstenii* as the dominant species. Higher abundances of *F. reinholdii* between 7.3 and 6.5 Ma and abundances of *Thalas-*

sionema nitzschioides up to 70% between 6.3 and 5.4 Ma suggest a warm-water influence (Fig. 4.7). *Thalassiosira oestrupii* occurred between 5.3 Ma and 4.5 Ma with abundances up to 6%. The cold-water indicating species *D. dimorpha* increased between ca. 9 and 7.3 Ma, but it is replaced by the dominant cold-water species *Fragilariopsis praecurta*, *F. arcula* and *F. aurica* at around 7 Ma (Fig. 4.7).

Relative low temperatures are estimated at Site 701 for the lower portion of the investigated Tortonian sediments (Fig. 4.8). The low amount of warm-water species combined with continuous presence of the cold-water taxa *D. dimorpha*, *F. donauhensis* and *F. praecurta* indicate cold surface water (Fig. 4.6). Early Messinian RPTs at Site 701 indicate even climatic conditions, which is documented mainly by the increased occurrence of warm-water taxa *T. nitzschioides* spp., *A. tabularis*, *A. ingens*, *A. ingens* var. *ovalis* and *F. reinholdii* (Fig. 4.6). Additionally, warm-water species *H. triangularus* occurred between ca. 7.3 and 6.5 Ma with mean abundances of 15%. A cooling event around 6.4 Ma is calculated from the abrupt extinction of *H. triangularus* in combination with an abundance peak of the cold-water taxa *F. praecurta*. Yet other cooling events are also documented around 5.8 and 5.5 Ma (Fig. 4.8). These estimates can be concluded from short-term increased abundances of cold-water species *F. aurica* and *F. praecurta* (Fig. 4.6)

Site 704 RPTs indicate generally warmer surface water conditions compared to Site 701. Distinct cooling events are documented at 8.5, 7.9, 7.6 Ma during the Tortonian stage and at 6.4 and 5.8 Ma during the Messinian. The latter coincides with cold events documented at Site 701 (Fig. 4.8). Calculation of the Tortonian cooling events (8.5, 7.9 and 7.6 Ma) resulted mainly from high abundances of *D. dimorpha* (Fig. 4.7). Starting at the uppermost Messinian, a general cooling is documented at Site 704. The occurrence of cold-water masses as indicated by RPTs is inferred from the strongly increased abundance values of the cold-water species *F. praecurta*. However, this latest Miocene/earliest Pliocene cooling is in contrast to RPT estimates from Site 701, where continuous stable temperatures are calculated (Fig. 4.8).

Late Miocene RPT curves calculated at Sites 689, 1088 and 1092 (Censarek and Gersonde, subm. b) are considered to reveal the latitudinal development of Southern Ocean water masses. Paleotemperatures at Site 689 indicate a temperature decrease between 9.5 and 8.6 Ma, which is not documented at any other site. However, the cooling started close to the Miocene/Pliocene boundary and is documented at Sites 689, 704 and 1092.

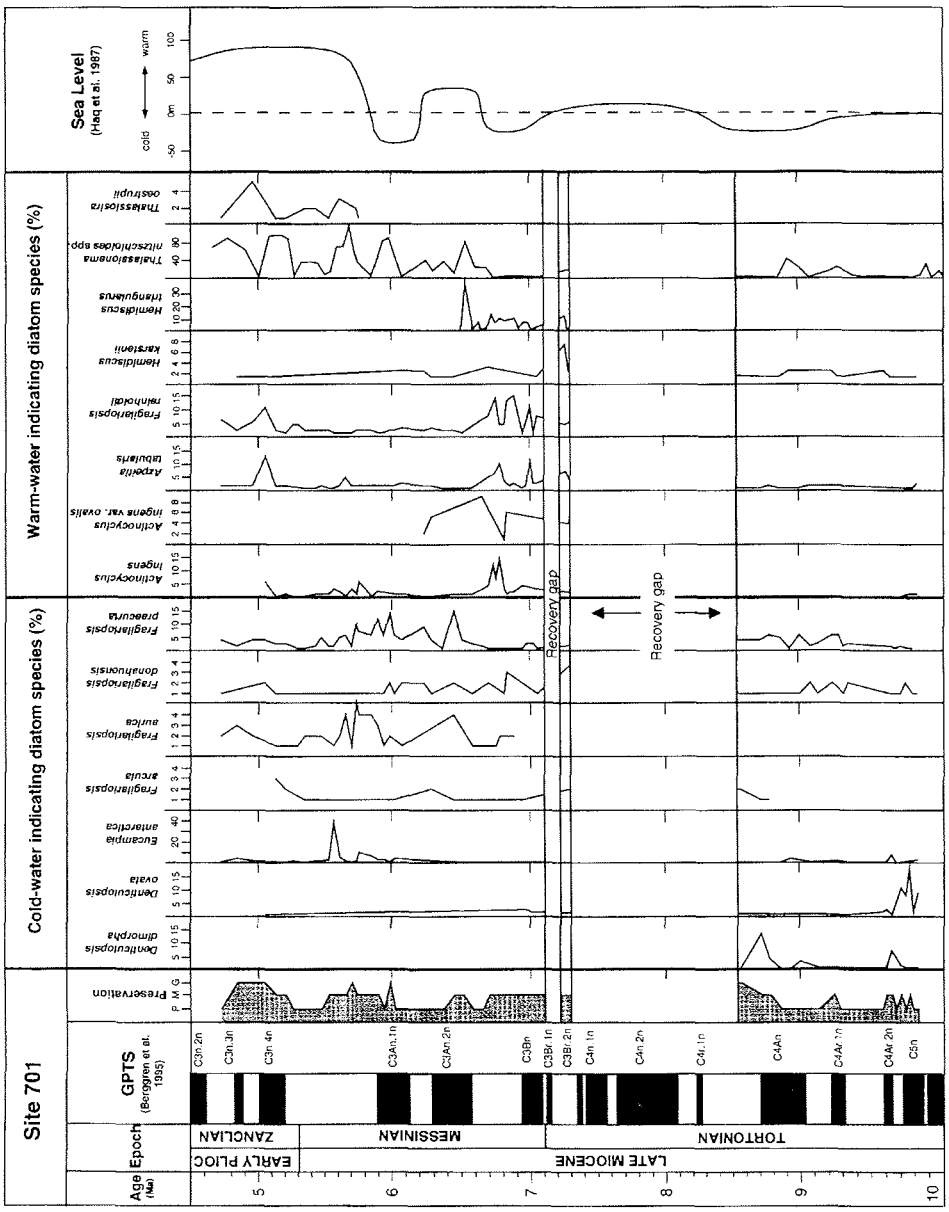

Figure 4.6: Late Miocene diatom abundance fluctuations of warm- and cold-water indicating species at Site 701 are presented. Diatom preservation (P: poor, M: moderate, G: good) refers to the degree of opal dissolution which have to be considered interpreting diatom data. The sea level curve (Haq et al., 1987) tied to the Geomagnetic Polarity Time Scale (GPTS) of Berggren et al. (1995) is presented

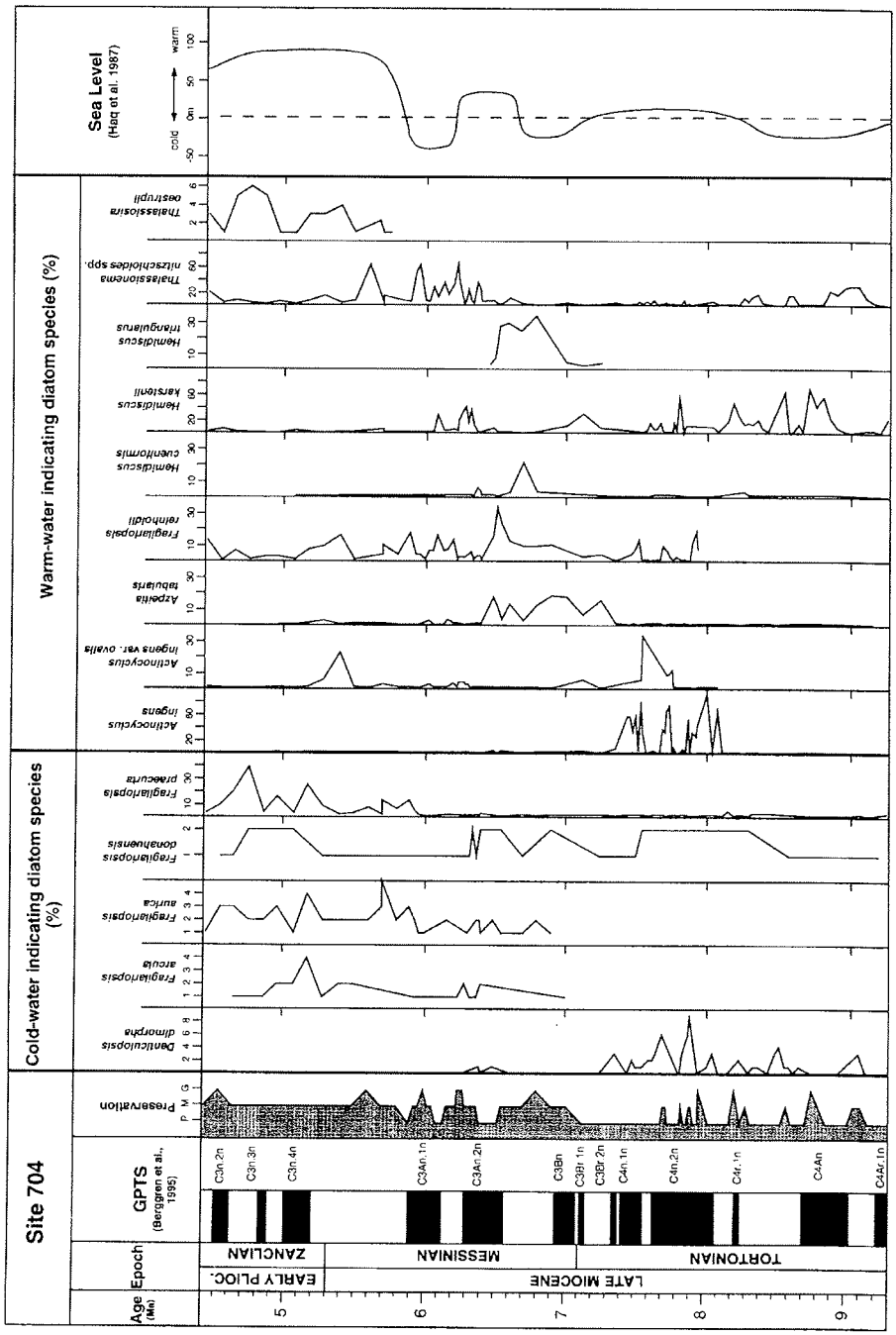

Figure 4.7: Late Miocene diatom abundance fluctuations of warm- and cold-water indicating species at Site 704 are presented. Diatom preservation (P: poor, M: moderate, G: good) indicate the degree of opal dissolution which have to be considered interpreting diatom data. The sea level curve (Haq et al., 1987) tied to the Geomagnetic Polarity Time Scale (GPTS) of Berggren et al. (1995) is presented.

RPTs estimated at nearby Sites 704 and 1092 reflect in general a comparable thermal water mass evolution (Fig. 4.8). Major events of the development of the Mediterranean Sea are compared to the climatic evolution of the Southern Ocean (Fig. 4.8). At a time when the Mediterranean basin was isolated from the Atlantic Ocean diatom concentrations at Sites 704 and 1092 reached highest values. During the period of evaporite deposition in the Mediterranean basin diatom concentrations at Sites 704 and 1092 stayed on this high level, showing minor flucuations, whereas at Site 701 a period of low values is documented (5.6 to 5.3 Ma). Paleotemperatures during this period occasionally indicate temporarily cold surface water conditions in the Southern Ocean. The onset of climate deterioration at Sites 701 and 704 can be assumed between 6.1 and 5.9 Ma, which temporally coincides with the progressive isolation of the Mediterranean basin (Fig. 4.8).

4.4.3 Thermal evidences from latitudinal abundance comparisons of selected diatom species

Abundance fluctuations of a cold-water indicating diatom (*Fragilariopsis praecurta*) three warm-water indicating species (*Hemidiscus triangularus*, *Azpeitia tabularis* and *Thalassiosira oestrupii*) and a warm-water indicating *Hemidiscus*-group consisting of *H. karstenii*, *H. cuneiformis* and *H.* sp. A (Gersonde and Burckle, 1990) reflect in detail the thermal development at Sites 701 and 704 (Fig. 4.9). Additionally abundance fluctuations of those species at Sites 689, 1088 and 1092 are considered.

A long-range warm surface water period is deduced from high abundances of *A. tabularis* and of the *Hemidiscus*-group between 7.3 and 6.6 Ma (Fig. 4.9). A cold period indicated primarily by increased abundances of *F. praecurta* (Site 701) and low abundances of *A. tabularis* and the *Hemidiscus*-group lasted until 5.6 Ma. Between 5.3 to ca. 4.5 Ma *F. praecurta* became common in the northern area of the Southern Ocean (Site 704). During the same period the warm-water species *T. oestrupii* occurred in this area. Increased abundances of *A. tabularis* at Sites 689 and 701 indicates a relative warming in the southern investigated area. Short-term cold periods are determined between 7.5 and 7.3, 8.9 and 6.8, 6.4 and 6.3, 6.2 and 6.1, 6 and 5.7, 5.1 and 5.15, 4.85 and 4.75 Ma (Fig. 4.9).

The cold-water indicating *F. praecurta* is closely related to the recent *F. curta*, probably being its phylogenetic precursor (Gersonde, 1991). *Fragilariopsis curta*

is used for the reconstruction of sea-ice extension in the Southern Ocean (Gersonde and Zielinski, 2000). A similar geographical abundance distribution of both species (Zielinski and Gersonde, 1997) and the continuous succession from *F. praecurta* to *F. curta*, somewhere between 3.5 and 4.2 Ma as documented at Leg 120 Holes 747B, 748B (Harwood and Maruyama, 1992), suggest that *F. praecurta* might had also an affinity to sea-ice. Therefore an increase in seasonal sea-ice coverage might be assumed between 6.6 and 5.4 Ma, documented at Site 701 (Fig. 4.9). Between 6.4 and 5.4 Ma the sediments at Maud Rise Site 689 are not preserved. Occurrences up to 30% of *F. praecurta* in the section younger than 5.4 Ma might refer to a stronger sea-ice occurrence. However, high abundances of this species at Sites 704 and 1092 during the Early Pliocene would indicate an unusual northward expansion of sea-ice.

A comparison of Miocene abundances of the extant species *A. tabularis* and *T. oestrupii* with their present-day abundance ranges (Zielinski and Gersonde, 1997) reveals the difference to recent surface water temperatures (Fig. 4.9).

Between 7.3 and ca. 6.6 Ma abundances of *A. tabularis* indicate warmer than present surface water temperatures at all sites. During the middle to late Messinian cold period similar or lower abundances than recent are documented (Fig. 4.9). In the earliest Pliocene at Sites 689 and 701 abundances of *A. tabularis* partly exceeded the present-day range of values, indicating warmer than recent temperatures. *T. oestrupii* occurred at around 5.6 Ma with average higher abundances than present-day at Site 701 and similar values at Sites 704 and 1092. Only in some periods of the early Pliocene abundances of *T. oestrupii* exceeded the present value range.

Mediterranean climatic development is indicated by the benthic isotope record of the Salé Briqueterie drill core (Hodell et al., 1994), recording ongoing cooling and a long-term cold period between 6.6 and ca. 5.5 Ma. It is subsequently followed by a warming period up to ca. 5.25 Ma (Fig. 4.9). A similar thermal development is suggested by the diatom record for the Southern Ocean.

Figure 4.8 (right): Relative paleotemperatures at Sites 701 and 704 and at Sites 689, 1088 and 1092 (Censarek and Gersonde, subm. b) reflect the relative thermal development of the Southern Ocean surface waters. Diatom concentrations supplement thermal interpretations. Grey fields mark the recent range of diatom abundance (after Zielinski and Gersonde, 1997). For comparison with the Mediterranean Sea climate development important events of the Messinian Salinity Crises are compiled (Hodell et al., 1994 and 2001; Krijgsman et al., 1999 and 2001).

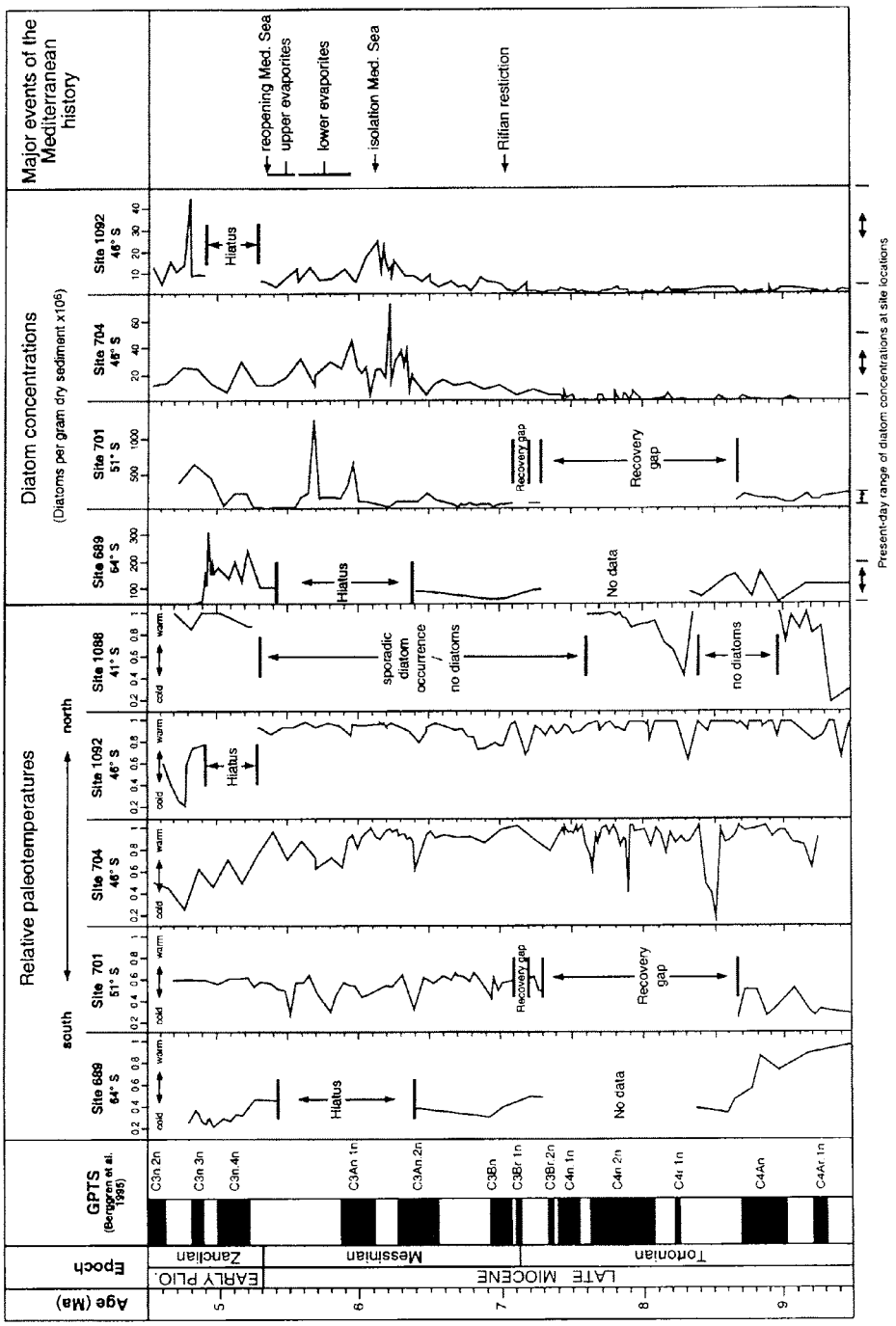
Major events of the Mediterranean history
reopening Med. Sea
upper evaporites
lower evaporites
isolation Med. Sea
Rifian restiction
Diatom concentrations
(Diatoms per gram dry sediment x10⁶)
Site 1092 46° S
Site 704 46° S
Site 701 51° S
Site 689 64° S
Hiatus
Recovery gap
Recovery gap
Hiatus
No data
Present-day range of diatom concentrations at site locations
Relative paleotemperatures
south
north
Site 689 64° S
Site 701 51° S
Site 704 46° S
Site 1092 46° S
Site 1088 41° S
cold
warm
Hiatus
Recovery gap
Recovery gap
Hiatus
No data
No data
sporadic diatom occurrence / no diatoms
no diatoms
GPTS (Berggren et al. 1995)
C3n 2n
C3n 3n
C3n 4n
C3An 1n
C3An 2n
C3Bn
C3Br 1n
C3Br 2n
C4n 1n
C4n 2n
C4r 1n
C4An
C4Ar 1n
Epoch
Zanclian
Messinian
Tortonian
EARLY PLIO.
LATE MIOCENE
Age (Ma)
5
6
7
8
9

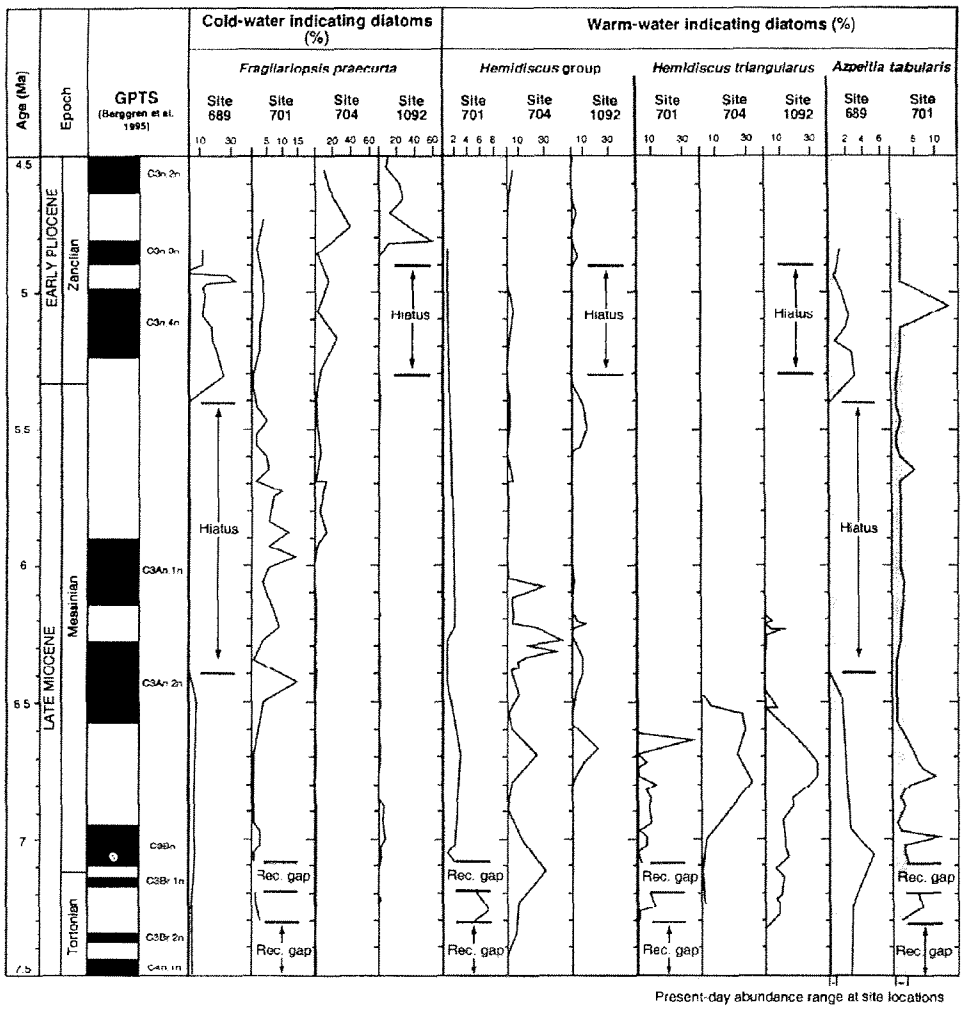

Figure 4.9 (both sides): Latitudinal comparison of abundances of selected diatom species indicating thermal conditions and deduced long-term and short-term climatic changes in the Southern Ocean. Abundance ranges of still recently occuring diatom species *A. tabularis* and *T. oestrupii* at site

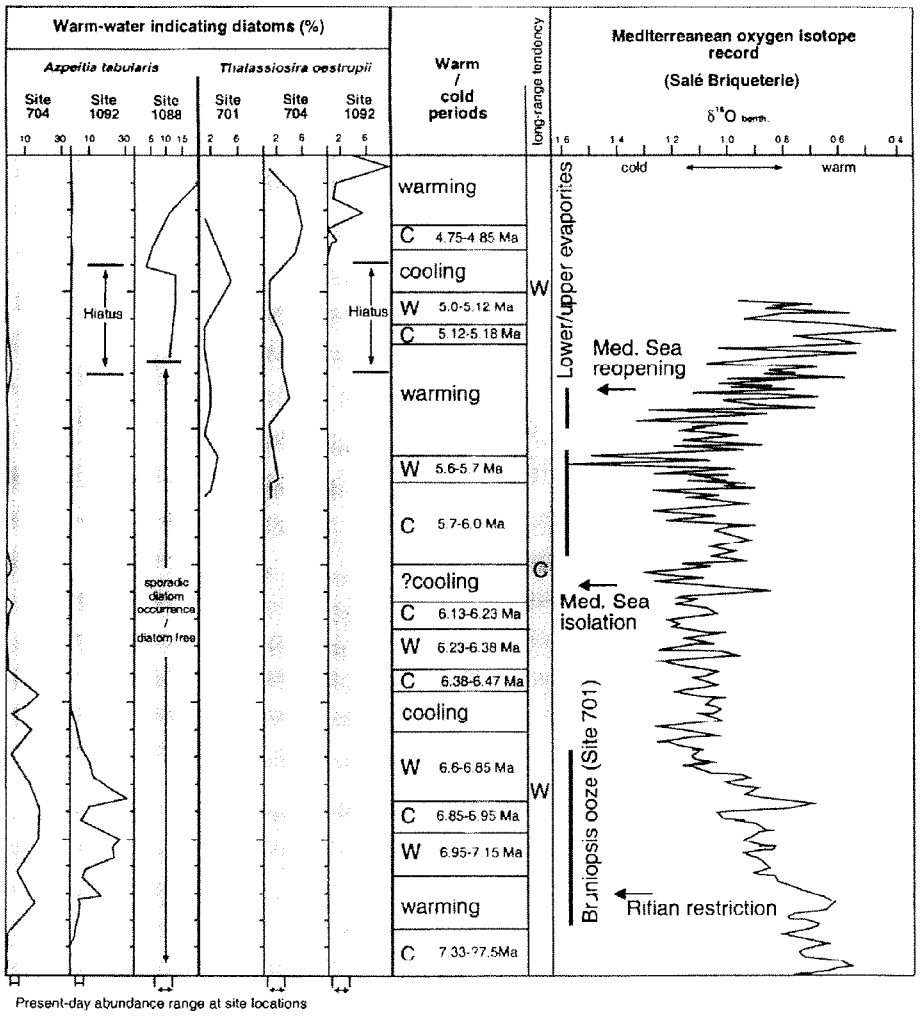

locations are marked as grey fields (after Zielinski and Gersonde, 1997). The Mediterranean oxygen isotope record from the Salé Briqueterie, northwestern Morocco (Hodell et al., 1994), shows a comparable climate development as the one deduced from diatom abundances.

Furthermore, during the isolation period of the Mediterranean Sea F. praecurta occurred for the first time at Site 704 with abundances up to 10% indicating a general cooling of Southern Ocean water masses. The end of the lower evaporite deposition (ca. 5.6 Ma) in the Mediterranean basin is succeeded temporally by the onset of relative warm Southern Ocean water masses indicated by T. oestrupii occurrences combined with decreasing abundances of F. praecurta.

4.5 Discussion and conclusions

4.5.1 Biostratigraphic remarks

Miocene diatom assemblages of southern Polar Front Zone Site 701 differ remarkably from those of the northern Polar Front Zone (Sites 704 and 1092). Therefore, different diatom assemblages within a single hydrographic zone have to be considered during further revisions of Southern Ocean diatom zonations. More than two diatom zonations will obviously be needed to improve the Latest Miocene diatom biostratigraphies. Furthermore, differences in assemblage composition within the Polar Front Zone imply that diatom linkage to hydrographical front conditions should be refined, e.g. during the application of factor analysis. It becomes obvious that hydrographic fronts are usually not strong boundaries of oceanographic parameters as they are often seen and that frontal zones represent not uniform hydrographic conditions.

Slight discrepancies in diatom assemblages found between Site 704 and closeby Site 1092 can attribute to different preservation conditions. These discrepancies occur when lightly silicified species (e.g. *F. aurica*, *F. arcula*) are involved. Sedimentation rates and diatom concentrations at Site 1092 are twice as high compared to Site 704 (Censarek and Gersonde, 2002), which indicates differences in sedimentation processes and preservation conditions.

This is the first investigation estimating a reliable FOD for *T. oestrupii* in the Atlantic sector of the Southern Ocean. It is placed at around 5.8 Ma (lower portion of Chron C3r) at both sites, which is the earliest datum compared to other partly uncertain occurrences (see discussion in Censarek and Gersonde, 2002). The absence of *T. oestrupii* below the hiatus (68.46 mcd) at Site 1092 is not yet understood (Censarek and Gersonde, 2002). The hiatus at Site 1092 comprises possibly slightly more time than calculated (4.9 to 5.3 Ma).

The ca. 25 m *Bruniopsis*-ooze at Site 701 is important for paleoclimate interpretation (Fig. 4.3). This warm-water taxa, which is mostly found in fragments, oc-

curred cosmopolitically during the Middle and Late Miocene (Schrader, 1973, 1974 and 1976). For the same time period a diatom-ooze consisting of *Ethmodiscus rex* is documented at South Atlantic Site 520 (Hsü et al., 1984), which made the Shipboard Scientific Party (1988c) speculate about a basin wide event throughout the South Atlantic. However, an ooze made of *Bruniopsis* sp. is only reported at Site 701. Below the Bruniopsis-ooze section a ca. 3 m thick sand/gravel unit is found, which might be explained as ice-rafted debris deposits (Shipboard Scientific Party, 1988c). Therefore, a cooling event might be assumed approximately between 8.7 and 7.3 Ma. Subsequently, an extraordinarily warm surface water mass would occur between ca. 7.3 and 6.68 Ma.

4.5.2 Miocene thermal history and evidences of hydrographic frontal displacements

The combination of a cold diatom assemblage at Site 689 between at least 9.5 and 8.6 Ma and a slight warming at the northern Sites 704, 1092 and 1088 (Fig. 4.8) implies a strengthening of thermal fronts. As cold conditions at the Maud Rise (Site 689) are established, a southernly located, weakly developed Paleo-Polar Front must be supposed (Fig. 4.10.A). The RPT calculations at Sites 689 and 701support the assumption that the temperatures between 8.6 and ca. 7.3 Ma were similar to the recent ones, which in turn indicates that the Paleo-Polar Front was located close to recent position (Fig. 4.10.B). Whereas lower than present diatom concentrations between 9.5 and 7.3 Ma at Sites 704, 1092 and a warm-water indicating diatom assemblage (Fig. 4.8) indicate a Paleo-Subantarctic Front location somewhat south of the present (Fig. 4.10.C). It is followed by a generally warmer than present period (7.3 to ca. 6.5 Ma) of surface water masses (Figs. 4.6, 4.7, 4.9 and 4.10.D). The *Bruniopsis*-ooze (Site 701) and abundances of *A. tabularis,* exceeding present day values at all sites (Fig. 4.9), support the interpretation of an extraordinarily warm period possibly coupled with a southward front displacement. Decreased abundances of warm-water indicating species between 6.85 and 6.95 Ma (Fig. 4.9) refer to a prominent cooling of surface waters, interrupting the warm period of the earliest Messinian. We speculate that frontal zones migrated for ca. 100 k.y. northward (Fig. 4.10.E). This cooling might be linked to the carbon isotope shift (lower portion of Chron C3Ar), which is proposed to be a result of an increased erosion from terrigenous and shelf sediments during sea level lowering caused by Antarctic glaciation (Berger and Vincent, 1986). The cold period (6.85 to 6.95 Ma) coincides with results of Hodell et al. (1994), who suggested an increase in

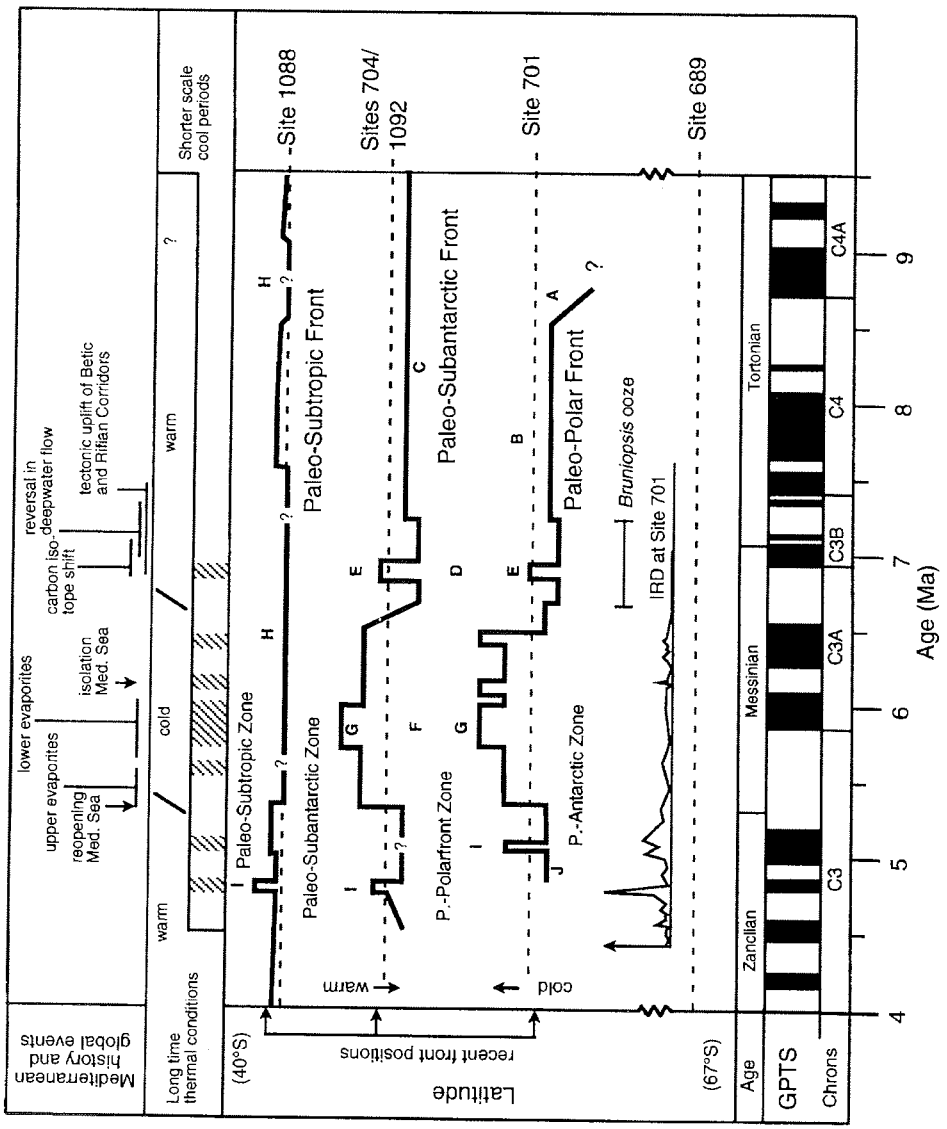

Figure 4.10: The sketch summarises estimated hydrographic front migragions relativ to site locations. Long time as well as short ranging thermal states as indicated by diatom abundance investigation are shown. Letters A to J mark the discussed interpretations. The geomagnetic polarity time scale (GTPS) is according to Berggren et al. (1995). Events of the Mediterranean history are compiled by Hodell et al. (1994 and 2001), Krijgsman et al. (1999 and 2001). The interpretation of a northward movement at Geomagnetic Chron C3Ar of hydrographic fronts up to north of the recent positions is supported by the first occrrence of IRD at Site 701 (Allen and Warnke, 1991).

continental ice volume at Site 846 (eastern Equatorial Pacific) based on oxygen isotope measurements. However, increasing oxygen isotope values during this period at North Atlantic Site 982 are interpreted to reflect a change in intermediate water temperatures and would therefore be unrelated to global ice volume (Hodell et al., 2001). A northward front system movement between ca. 6.5 and 5.3 Ma is indicated by high abundances of the cold-water species *F. praecurta* and low abundances of the warm-water species (Figs. 4.8, 4.9, 4.10.F).

Paleo-Polar Front Zone conditions might have occured on the Meteor Rise due to a northward movement of Paleo-Subantarctic Front. The interpretation of the strong northward movement beyond Site 701 location is supported by the onset of ice rafted debris (IRD) at Site 701 (Allen and Warnke, 1991; Warnke et al., 1992). First IRD occurred in the uppermost portion of Chron C3Ar corresponding to an age of ca. 6.6 Ma.

During the late Messinian cold period (6.5 to 5.3 Ma) three prominent colder intervals could be determined (Fig. 4.9), ranging from ca. 6.38 to 6.47 Ma, 6.13 to 6.23 Ma and 5.7 to 6.0 Ma, which might indicate a northward front migration (Fig. 4.10.G). Hodell et al. (2001) described 18 glacial/interglacial cycles during this period, inferred from oxygen isotope studies at Site 982 (North Atlantic). The occurrence of *T. oestupii*, decreasing *F. praecurta* abundances and RPTs (Fig. 4.8, 4.9) indicate a short-term warm interval between ca. 5.6 and 5.7 Ma, which is in good agreement with isotopic studies at Site 588 (Southwest Pacific) presented by Hodell et al. (1986). In the North Atlantic at Site 982 an interglacial event is also documented by low $\delta^{18}O$ values enclosed by two prominent glacial stages named TG 20 at 5.7 Ma and TG 12 at 5.51 Ma (Hodell et al., 2001). This was probably the warmest stage during the Messinian glaciation history. Undoubtedly Site 1088 was influenced between 9.3 and 4.4 Ma by Subantarctic Front-Zone-like conditions. The almost diatom free sections and a higher carbonate content up to 93% between 9 and 8.4 Ma and between 7.6 and ca. 5.3 Ma might reflect an influence of a warmer Subtropical Zone-like surface water mass (Shipboard Scientific Party, 1999a) (Fig. 4.10.H). However, this implies a southward frontal migration during general cold periods with northward-displaced surface waters.

Diatom abundance fluctuations suggest cooler conditions around 5.15 and 4.8 Ma (Fig. 4.8, 4.9). Further evidence for a northward displacement of water masses during these stages and particularly for the time around 4.8 Ma, came from decreasing RPTs and from high diatom concentrations (Figs. 4.8, 4.9, 4.10.I). The cold period at 4.8 Ma is also documented by a prominent ice-rafted

detritus peak reported at Kerguelen Sites 745 and 746 (Ehrmann et al., 1991; Barron et al., 1991). Burckle et al. (1992) have evidence for a major glaciation in Chron C3n2r (ca. 4.7-4.8 Ma) of Hole 737A. They interpreted low percentages of opal combined with low (Ge/Si)-opal values as a glacial event at this site, which is located close to the present Polar Front. Yet, in general the Early Pliocene is characterized by decreasing diatom concentrations and occurrences of typical warm-water taxa. Higher than present-day abundances of *T. oestrupii* at Sites 701, 704 and 1092 (Fig. 4.9) refer to a strong warming and imply consequently a southward displacement of the Paleo-Polar Front Zone (Fig. 4.10.J). This warming period is also documented by the occurrence of calcareous nannofossil assemblages at Kerguelen Sites 744 and 737 (Wei and Thierstein, 1991). Bohaty and Harwood (1998) estimate a temperature difference of at least 4°C at Sites 748 and 751 for the southern Kerguelen Plateau surface waters at 4.3 and 4.5 Ma, providing an idea of differences between Early Pliocene thermal states.

4.5.3 Evidences of triggering and steering of the Messinian Salinity Crisis (MSC)

A combination of tectonic and glacio-eustatic processes are proposed to cause isolation, desiccation and reopening of the Mediterranean basin and to initiate and control the MSC (Kastens, 1992; Benson et al., 1991; Hodell et al., 1994, 2001; Krijgsman et al., 1999, 2001; Vidal et al., 2001). Continental ice volume accumulation, mainly in Antarctica, but also on the Northern Hemisphere lowered the eustatic sea level (Haq et al., 1987; Larsen et al., 1994). Our study documents for the first time the Southern Ocean thermal development during the Messinian, providing evidences for the cryospheric evolution in Antarctica. In general a synchron thermal development of the Southern Ocean and the Mediterranean Sea is documented (Figs. 4.8, 4.9, 4.10). Reconstructed RPTs at Sites 701 and 704 reflect a long-range Southern Ocean cooling from 6.3 Ma to 5.9 Ma terminating in a cold period until 5.7 Ma (Fig. 4.8). Increased abundances of *F. praecurta* at ca. 5.9 Ma at Site 704 document the northward expansion of cold-water masses (Fig. 4.9), which refers indirectly to increasing Antarctic ice volume and sea level lowering during the period of Mediterranean isolation and onset of lower evaporite deposition. This interpretation is supported by reduced abundances of warm-water indicating diatoms at this time. In contrast a rapid deglaciation and coupled sea level rise could not be deduced from the estimated thermal record for the period around the Mediterranean re-

opening (5.33 Ma). Therefore an explicit influence of glacio-eustatic processes can be supposed for the onset of the MSC, but not for the termination. However, the slowly proceeding warming at the Miocene/Pliocene boundary would undoubtedly rise the sea level.

This result coincides in general with the interpretation of oxygen isotope studies by Hodell et al. (1994, 2001). The increase in the benthic oxygen isotope signal in the Salé Briqueterie core (Fig. 4.9) is interpreted, at least in part, as an increase in global ice volume that lowered the sea level (Hodell et al., 1994). This conclusion is based on the 41-kyr cycle of orbital obliquity, which suggests that the oxygen isotope signal was partly controlled by changes in continental ice volume that were responding to insolation changes at high latitudes. At North Atlantic Site 982 Hodell et al. (2001) revealed 18 glacial-to-interglacial oscillations. There is evidence for a strengthened glaciation just before the onset of lower evaporite deposition in the Mediterranean. From our data reflooding of the Mediterranean basin can not be attributed to a single rapid thermal event, which suggests that tectonic changes were the main cause for the termination of the MSC (Hodell et al., 2001).

Some studies proposed regional tectonic changes as the dominant factor for the isolation of the Mediterranean basin, which contrasts the results shown in Hodell et al. (1994) and herein. Reason for this discrepancies are (i) interpretations of the 41-yr orbital obliquity isotope values as deep-sea temperature-effect (Shackleton and Crowhurst, 1997) and (ii) differences between timing of orbitally tuned isotope events and the chronology of geological features at the Mediterranean basin (Krijgsman et al., 1999; Vidal et al., 2001).

Considering the difficulties in oxygen isotope measurement interpretations, paleoecological diatom studies, as presented in this article, are a useful, independent tool to unravel the evolving discrepancies. A higher temporal resolution of Site 701 and 704 would enable a more detailed comparison of Southern Ocean thermal stages and the geological features of Mediterranean to reveal the influence of ice volume changes on the MSC.